



The following Communications have been judged by at least two referees to be “very important papers” and will be published online at www.angewandte.org soon:

K. Ohmori, T. Shono, Y. Hatakoshi, T. Yano, K. Suzuki*
An Integrated Synthetic Strategy for Higher Catechin Oligomers

K. Nakano, S. Hashimoto, M. Nakamura, T. Kamada, K. Nozaki*
Synthesis of Stereogradient Poly(propylene carbonate) by Stereo- and Enantioselective Copolymerization of Propylene Oxide with Carbon Dioxide

X. Wurzenberger, H. Piotrowski, P. Klüfers*
A Stable Square-Planar High-Spin- d^6 Molecular $\text{Fe}^{\text{II}}\text{O}_4$ Chromophore From Rare Iron(II) Minerals

I. Piel, M. Steinmetz, K. Hirano, R. Fröhlich, S. Grimme,*
F. Glorius*
Highly Asymmetric NHC-Catalyzed Hydroacylation of Unactivated Alkenes and Mechanistic Insights

Y. Han-ya, H. Tokuyama, T. Fukuyama*
Total Synthesis of (–)-Conophylline and (–)-Conophyllidine

N. Dietl, C. van der Linde, M. Schlangen, M. K. Beyer, H. Schwarz*
The Final Piece in an Intriguing Puzzle: Diatomic $[\text{CuO}]^+$ and Its Role in Spin-Selective Hydrogen- and Oxygen-Atom Transfer in the Thermal Activation of Methane

I. Garcia-Bosch, A. Company, C. W. Cady, S. Styring, W. R. Browne, X. Ribas, M. Costas*
Evidence for a Precursor Complex in C–H Hydrogen-Atom-Transfer Reactions Mediated by a Manganese(IV) Oxo Complex

G. N. Newton, S. Yamashita, K. Hasumi, J. Matsuno, N. Yoshida, M. Nihei, T. Shiga, M. Nakano, H. Nojiri, W. Wernsdorfer, H. Oshio*
Redox-Controlled Optimization of the Magnetic Properties of Keggin-Type $\{\text{Mn}_{13}\}$ Clusters

I. Nischang,* O. Brüggemann, I. Teasdale
Facile, Single-Step Preparation of Versatile, High-Surface-Area, Hierarchically Structured Hybrid Materials

Author Profile



“My favorite piece of research is Emil Fischer’s beautiful work on the hexoses.
When I was eighteen I wanted to move to and live in Spain (it just took me another 20 years to see it through) ...”
This and more about Kilian Muñiz can be found on page 4260.

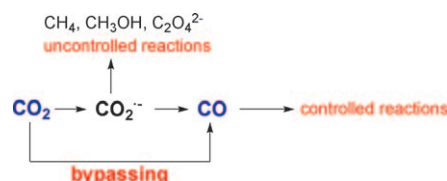
Kilian Muñiz ————— 4260

Highlights

CO_2 Reduction

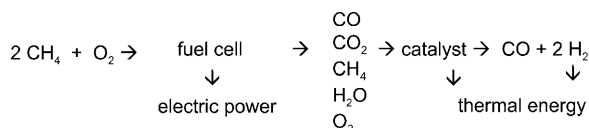
U.-P. Apfel,* W. Weigand* — 4262 – 4264

Efficient Activation of the Greenhouse Gas CO_2



CO₂, can do: Recently, two groups independently described elegant ways for the direct two-electron reduction of CO_2 to CO, bypassing the formation of the $\text{CO}_2^{\bullet-}$ radical (see scheme). Armstrong et al. used a photoactive Ru complex and the

CO_2 -reducing enzyme CODH I immobilized on TiO_2 nanoparticles. Cummins et al. exploited a Nb^{V} nitrido complex in which the nitrido ligand reacts with CO_2 to give a carbamate species.



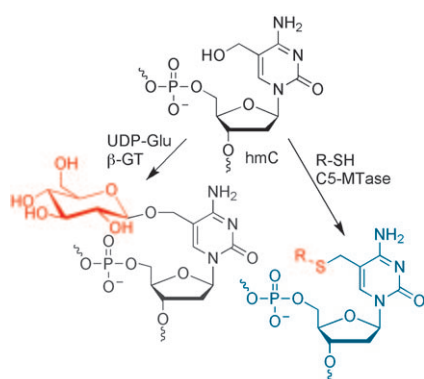
No coking is observed in a single-chamber fuel cell in which CH_4 and O_2 are converted into a mixture of H_2O , CO , H_2 , CH_4 , CO_2 , and O_2 ; electric power is generated and the product gas mixture is passed over a syngas catalyst, which generates

heat and forces the mixture to thermodynamic equilibrium. The advantages of this setup over the direct conversion of CH_4 and O_2 into syngas at higher temperatures are the generation of electric power and the improved reactor safety.

Single-Chamber Fuel Cells

W. F. Maier* _____ 4265 – 4267

Electric Power and Syngas from Methane—An Energy-Efficient Combination of a Single-Chamber Fuel Cell and Downstream Catalytic Equilibration



New methods for the chemoenzymatic derivatization of 5-hydroxymethylcytosine (hmC) utilize bacteriophage β -glycosyltransferase (β -GT) or an unexpected activity of bacterial cytosine 5-methyltransferases (C5-MTase) to install reactive functional groups on the hydroxymethyl group for detection, quantification, affinity enrichment, and analysis of the recently discovered epigenetic hmC modification in mammalian DNA.

DNA Modification

C. Höbartner* _____ 4268 – 4270

Enzymatic Labeling of 5-Hydroxymethylcytosine in DNA



Porphyrins may be confused, but Linus Pauling and Melvin Calvin were not! Calvin proposed “carboporphyrins” in 1943 and, unbeknownst to contemporary science, Pauling contemplated the existence and stability of such fundamental porphyrin isomers in 1944. What he called “isoporphyrins” with “extroverted pyrrole rings”, nowadays called N-confused porphyrins, were discovered 50 years later in 1994 by Furuta and Latos-Grażyński et al.

Essays

Porphyrin Isomers

M. O. Senge* _____ 4272 – 4277

Extroverted Confusion—Linus Pauling, Melvin Calvin, and Porphyrin Isomers

For the USA and Canada: ANGEWANDTE CHEMIE International Edition (ISSN 1433-7851) is published weekly by Wiley-VCH, PO Box 191161, 69451 Weinheim, Germany. Air freight and mailing in the USA by Publications Expediting Inc., 200 Meacham Ave., Elmont, NY 11003. Periodicals

postage paid at Jamaica, NY 11431. US POSTMASTER: send address changes to *Angewandte Chemie*, Journal Customer Services, John Wiley & Sons Inc., 350 Main St., Malden, MA 02148-5020. Annual subscription price for institutions: US\$ 9442/8583 (valid for print and electronic / print or electronic delivery); for

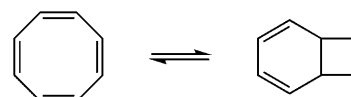
individuals who are personal members of a national chemical society prices are available on request. Postage and handling charges included. All prices are subject to local VAT/sales tax.

Eye-Witness Accounts

E. Vogel* — 4278–4287

From Small Carbocyclic Rings to
Porphyrins: A Personal Account of 50
Years of Research

An Eldorado of compounds is available from cyclooctatetraene, a compound notable for its ability to undergo valence isomerization. This eye-witness account of the development of their chemistry shows how interconnected the various areas of this fascinating research field are.



Reviews

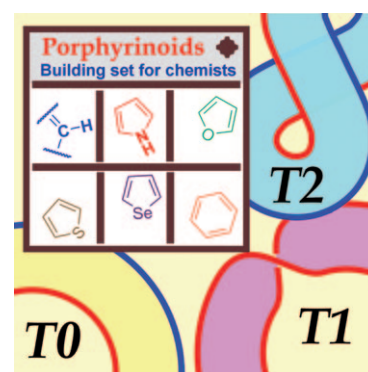
Porphyrinoids

M. Stępień,* N. Sprutta,
L. Latos-Grażyński* — 4288–4340



Figure Eights, Möbius Bands, and More:
Conformation and Aromaticity of
Porphyrinoids

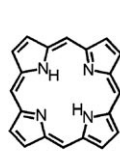
Incredibly elastic, superbly π -conjugated—and how colorful! Playing with porphyrinoids can be a grand pastime for any aromaticity-loving chemist. This exciting building set now contains not only pyrroles and methine bridges but also a variety of other hetero- and carbocycles. Snap a few π -bonds in place and you can make not only nature's favorite macrocycle but also, if you are adventurous, numerous topologically nontrivial rings.



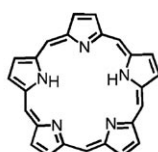
Porphyrinoids

S. Saito, A. Osuka* — 4342–4373

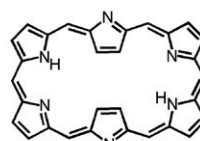
Expanded Porphyrins: Intriguing
Structures, Electronic Properties, and
Reactivities



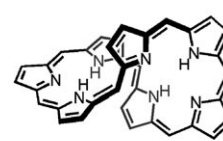
porphyrin



pentaphyrin



hexaphyrin



heptaphyrin

Higher homologues of porphyrins possess many interesting chemical and physical properties. These expanded porphyrins, which are macrocycles formed from pyrrole units (see scheme), show topologically different conformations and

aromatic/antiaromatic conjugated π -electron systems, and can undergo redox reactions and chemical modifications. The macrocycles can also bind one or more metal ions.

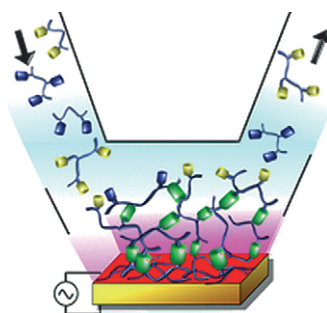
Communications

Film Formation

G. Rydzek, L. Jierry, A. Parat,
J.-S. Thomann, J.-C. Voegel, B. Senger,
J. Hemmerlé, A. Ponche, B. Frisch,
P. Schaaf,* F. Boulmedais — 4374–4377

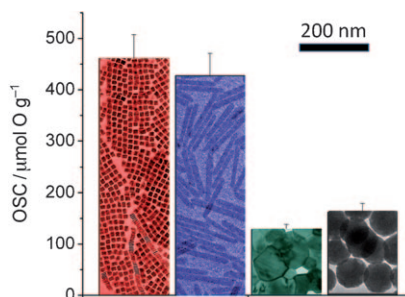


Electrochemically Triggered Assembly of
Films: A One-Pot Morphogen-Driven
Buildup



Polymers that “click”: A polymer film is obtained by the Cu^{I} -catalyzed Sharpless click reaction between two polymers, bearing either azide or alkyne groups, both present simultaneously in a Cu^{II} solution (see picture). The Cu^{I} morphogen is generated at an electrode by applying an adequate potential. This concept can be extended to supramolecular films formed by coordination complexes.

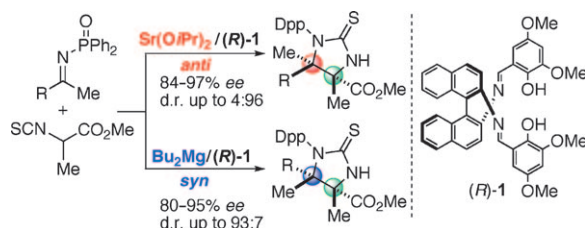
Small plate structure makes big difference: A facile synthetic method for high-quality ceria nanoplates enclosed by {100} facets involves the usage of a mineralizer. Compared to the 3D ceria nanomaterials prepared by combustion and hydrothermal treatment, the ceria nanoplates exhibit superior oxygen storage properties (see picture).



CeO₂ Nanoplates

D. Y. Wang, Y. J. Kang, V. Doan-Nguyen, J. Chen, R. Küngas, N. L. Wieder, K. Bakhmutsky, R. J. Gorte, C. B. Murray* 4378–4381

Synthesis and Oxygen Storage Capacity of Two-Dimensional Ceria Nanocrystals



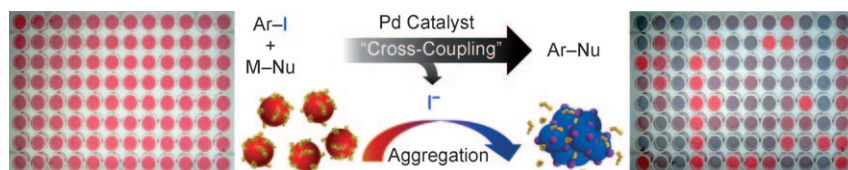
Now accessible: Sterically hindered vicinal tetrasubstituted carbon stereocenters, which are not accessible by asymmetric hydrogenation, were constructed by a catalytic asymmetric C–C bond formation

(see scheme; Dpp = diphenylphosphino). By changing the Group 2 metal center, stereodivergent access to α,β -tetrasubstituted α,β -diamino esters was realized.

Asymmetric Synthesis

G. Lu, T. Yoshino, H. Morimoto, S. Matsunaga,* M. Shibasaki* 4382–4385

Stereodivergent Direct Catalytic Asymmetric Mannich-Type Reactions of α -Isothiocyanato Ester with Ketimines



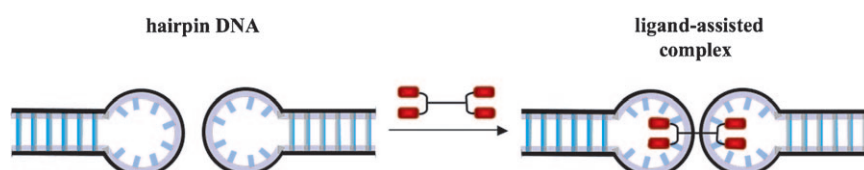
Catching the couplings: A general and simple screening method for palladium-catalyzed coupling reactions of aryl iodides utilizes gold nanoparticles. This

assay was successfully employed in several aminations, α -arylation of ketones, and decarboxylative couplings. 96 samples were screened in a few minutes.

Colorimetric Assays

E. Jung, S. Kim, Y. Kim, S. H. Seo, S. S. Lee, M. S. Han,* S. Lee* 4386–4389

A Colorimetric High-Throughput Screening Method for Palladium-Catalyzed Coupling Reactions of Aryl Iodides Using a Gold Nanoparticle-Based Iodide-Selective Probe



All loopy: The interaction of a series of mismatch-binding molecules with hairpin DNA that contains a d(CGG)₃ sequence in the loop is described (see picture). Native polyacrylamide gel electrophoresis of hairpin-loop DNA shows that the newly

synthesized mismatch-binding molecule, a tetrameric form of *N*-methoxycarbonyl-1,8-naphthyridine, assists the formation of a loop–loop complex of two DNA hairpin loops.

DNA Interactions

C. Hong, M. Hagihara, K. Nakatani* 4390–4393

Ligand-Assisted Complex Formation of Two DNA Hairpin Loops

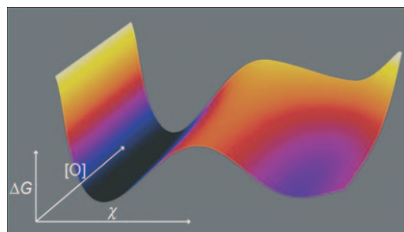


Protein Folding

D. Aioanei, S. Lv, I. Tessari, A. Rampioni,
L. Bubacco, H. Li, B. Samori,
M. Brucalé* ————— 4394 – 4397



Single-Molecule-Level Evidence for the
Osmophobic Effect



Chemical chaperones: Protecting osmo-lytes play a crucial role in preventing protein denaturation in harsh environmental conditions of living organisms. Experimental evidence is provided for a mechanism of protein-fold stabilization by these molecules that is in accord with the hypothesis of a backbone-based osmophobic effect. (In picture: ΔG = free energy, $[O]$ = osmolyte concentration, χ = unfolding reaction coordinate.)

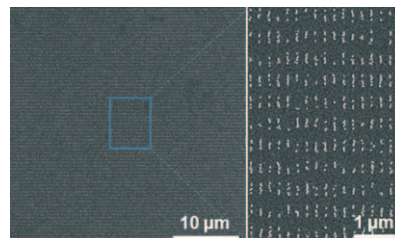
Nanofabrication

Y. H. Zheng, C. H. Lalander,
T. Thai, S. Dhuey, S. Cabrini,
U. Bach* ————— 4398 – 4402



Gutenberg-Style Printing of Self-Assembled Nanoparticle Arrays:
Electrostatic Nanoparticle Immobilization
and DNA-Mediated Transfer

Hot off the press: A Gutenberg-style nanoprinting technique that exploits electrostatic nanoparticle assembly and DNA-mediated replication of lithographically defined nanostructures was developed (see picture). Dense nanoparticle loading and high transfer yields were observed over three consecutive printing cycles, proving the potential to fabricate nanoparticle-based devices at low cost.

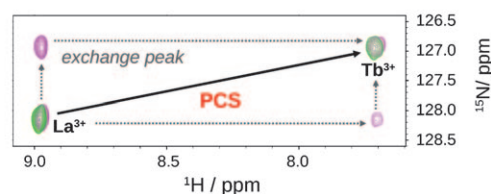
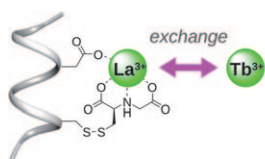


Lanthanide Tags

J. D. Swarbrick,* P. Ung,
S. Chhabra, B. Graham* — 4403 – 4406



An Iminodiacetic Acid Based Lanthanide
Binding Tag for Paramagnetic Exchange
NMR Spectroscopy



All the way with IDA! Attachment of iminodiacetic acid (IDA) to a protein helix creates a rigid lanthanide binding site that can be exploited for paramagnetic NMR spectroscopy (see picture). Pseudo-contact shifts (PCSs) larger than 8 ppm are

achievable with the tag, and metal exchange is sufficiently fast to enable signal assignment by $^{15}\text{N}_z$ exchange spectroscopy, eliminating the need for an initial protein model.

Cellular Imaging

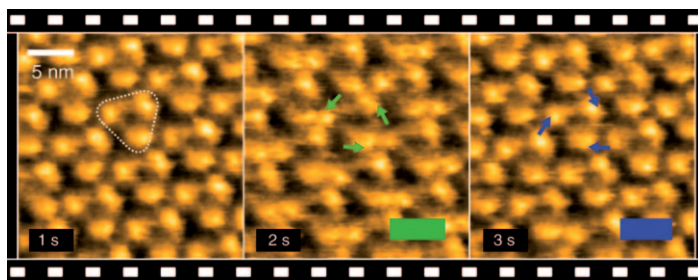
L. Yao, S. Xu* ————— 4407 – 4409

Force-Induced Remnant Magnetization
Spectroscopy for Specific Magnetic
Imaging of Molecules



FIRM evidence: Force-induced remnant magnetization spectroscopy (FIRMS) is developed to achieve molecular specificity in magnetic imaging. The method measures the magnetization of the magnetic particles as a function of an external

disturbing force. As the force-dissociated magnetic particles have no contribution to the signal, the binding force serves as a spectroscopic parameter for specific molecular and cellular identification (see picture).



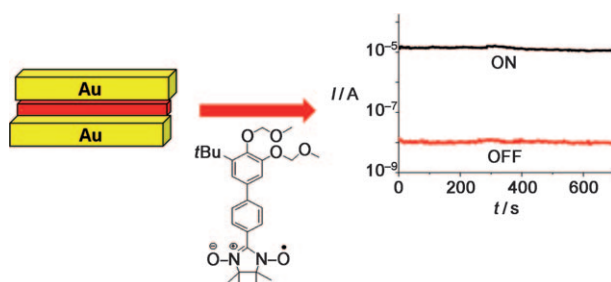
Blue light, green light: High-speed atomic force microscopy visualized light-induced structural changes of the D96N bacteriorhodopsin (bR) mutant under alternate two-color illumination. With green light,

each bR molecule is displaced outward from the trimer center. This activated structure is driven back to the ground state by the subsequent blue-light illumination (see picture).

Real-Time Atomic Force Microscopy

M. Shibata, T. Uchihashi, H. Yamashita, H. Kandori, T. Ando* — 4410–4413

Structural Changes in Bacteriorhodopsin in Response to Alternate Illumination Observed by High-Speed Atomic Force Microscopy



Can't fight the SEEPR: Simultaneous electrochemical electron paramagnetic resonance reveals that a molecule containing the nitronyl nitroxide (NN) radical (structure and red layer) is redox-active,

with switchability between oxidized and reduced states. An organic NN radical device utilizes the dual p- and n-type properties in a memory device.

Molecular Electronics

J. Lee, E. Lee, S. Kim, G. S. Bang, D. A. Shultz,* R. D. Schmidt, M. D. E. Forbes, H. Lee* — 4414–4418

Nitronyl Nitroxide Radicals as Organic Memory Elements with Both n- and p-Type Properties



DNA weaves a braided pattern: Two DNA single strands with mixed D- and L-nucleotides combine to weave a braided toroidal link. 5',5' linkages (fused circles)

and 3',3' linkages (bow-tie structures) are needed to maintain the strand polarity. Properly placed L-nucleotides are needed to achieve the woven pattern.

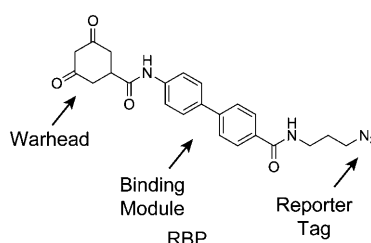
DNA Nanotechnology

T. Ciengshin, R. Sha, N. C. Seeman* — 4419–4422

Automatic Molecular Weaving Prototyped by Using Single-Stranded DNA



Three in one: The design strategy for redox-based probes (RBPs) that detect the reversible oxidation of protein tyrosine phosphatases (PTPs) includes a “warhead” that forms a covalent adduct with the oxidized active site cysteine of PTPs, a synthetic module that directs binding to the PTP active site, and a chemical reporter tag used for the identification, purification, or direct visualization of the probe-labeled proteins (see picture).



Chemoselective Redox Probes

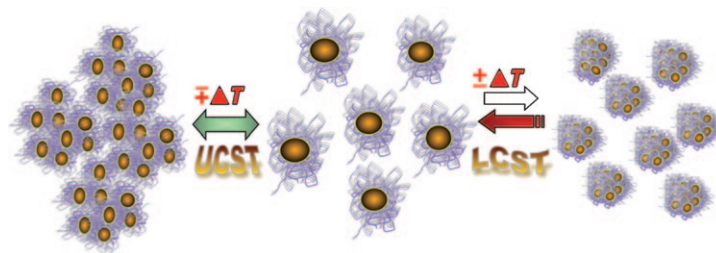
S. E. Leonard, F. J. Garcia, D. S. Goodsell, K. S. Carroll* — 4423–4427

Redox-Based Probes for Protein Tyrosine Phosphatases



Protein Engineering

N. K. Dutta,* M. Y. Truong, S. Mayavan,
N. Roy Choudhury,* C. M. Elvin, M. Kim,
R. Knott, K. M. Nairn,
A. J. Hill ————— 4428–4431



A Genetically Engineered Protein
Responsive to Multiple Stimuli

Smart protein: Careful design can yield novel biologically inspired materials that display advanced responsive behavior. A genetically engineered elastic protein dis-

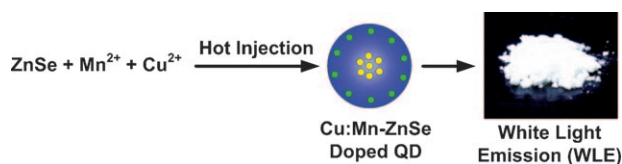
plays both a lower and an upper critical solution temperature (LCST and UCST, see picture), and its photophysical behavior depends on solution pH value.

Doubly Doped Nanocrystals

S. K. Panda, S. G. Hickey,*
H. V. Demir, A. Eyichmüller — 4432–4436



Bright White-Light Emitting Manganese
and Copper Co-Doped ZnSe Quantum
Dots



Doubly doped quantum dots with highly efficient (17%) white-light emission (WLE) have been directly synthesized using a one-pot hot-injection technique (see picture). The generation of WLE was

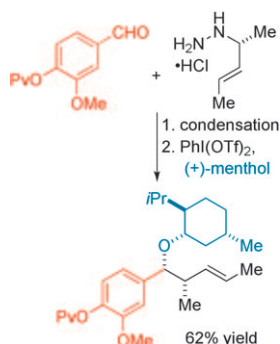
due to the judicious manipulation of the synthesis strategy for the co-doping of the host material—ZnSe quantum dots—with Mn and Cu.

Synthetic Methods

K. E. Lutz, R. J. Thomson* — 4437–4440



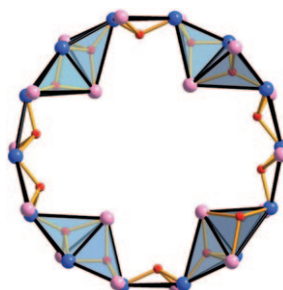
A Hypervalent Iodide-Initiated Fragment
Coupling Cascade of *N*-Allylhydrazones



Highway to the hydrazone: A hypervalent iodide initiated cascade process enables the rapid union of an aldehyde, an allylic hydrazide, and an alcohol (see scheme; Pv = pivaloyl). This process affords a diverse range of functionalized ether adducts, while simultaneously generating a stereodefined alkene and two new vicinal stereocenters. The use of chiral non-racemic hydrazines and alcohols offers a rapid entry to complex “natural product-like” structures.

Single-Molecule Magnets

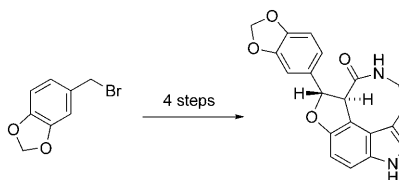
M. Manoli, R. Inglis, M. J. Manos,
V. Nastopoulos, W. Wernsdorfer,
E. K. Brechin,*
A. J. Tasiopoulos* ————— 4441–4444



A [Mn₃₂] Double-Decker Wheel

Inventing the double wheel: A mixed-valent [Mn₃₂] cluster with a very rare “double-decker” wheel topology (see its metal–oxygen core: Mn^{III} blue, Mn^{II} pink, O red) is reported. It is by far the highest-nuclearity example of its type, and it displays SMM behavior with the largest effective barrier to magnetization relaxation ($U_{\text{eff}} \approx 44.5$ K) for any molecular wheel.

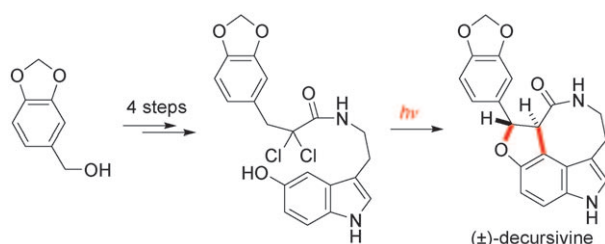
A four-step synthesis of the extracyclic, antimalarial indole natural product decursivine is described starting from commercial piperonyl bromide and serotonin (see scheme). A photoinitiated reaction cascade involving indole radical cation formation, rearrangement, radical recombination, rearomatization, elimination, and diastereoselective auto-acid-catalyzed closure of the dihydrofuran ring combine in a single step to conclude this remarkably efficient synthesis.



Decursivine

M. Mascal,* K. V. Modes,
A. Durmus _____ 4445–4446

Concise Photochemical Synthesis of the Antimalarial Indole Alkaloid Decursivine



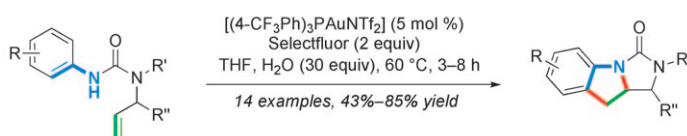
A photo op: The concise total syntheses of (±)-decursivine and (±)-serotobenine were achieved by using the titled cascade reaction, which is modeled on the bio-

mimetic pathway. The synthesis of (±)-decursivine, which exhibits antimalarial activity, was carried out in five steps without using protecting groups.

Decursivine

H. Qin, Z. Xu, Y. Cui, Y. Jia* 4447–4449

Total Synthesis of (±)-Decursivine and (±)-Serotobenine: A Witkop Photocyclization/Elimination/O-Michael Addition Cascade Approach



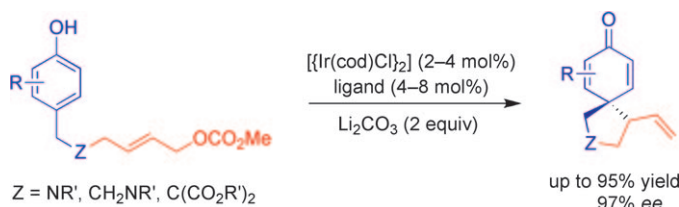
Gold rush: A combination of oxidative gold(I)/gold(III) catalysis and C–H functionalization led to the first oxidative coupling between in situ generated alkyl gold reagents and C_{sp²}–H bonds, affording tricyclic indolines through a formal

[3+2] annulation between a vinyl group and an aniline moiety [see scheme; Tf = trifluoromethanesulfonyl, Selectfluor = 1-chloromethyl-4-fluoro-1,4-diazoniabicyclo[2.2.2]octane bis(tetrafluoroborate)].

Nitrogen Heterocycles

G. Zhang, Y. Luo, Y. Wang,
L. Zhang* _____ 4450–4454

Combining Gold(I)/Gold(III) Catalysis and C–H Functionalization: A Formal Intramolecular [3+2] Annulation towards Tricyclic Indolines and Mechanistic Studies



Aromaticity lost: In the presence of [Ir(cod)Cl]₂ and a binol-derived phosphoramidite ligand, spirocyclohexadienone derivatives were obtained with up to

97% ee through iridium-catalyzed intramolecular asymmetric allylic dearomatization of phenols (see scheme; cod = cycloocta-1,5-diene).

Asymmetric Dearomatization

Q.-F. Wu, W.-B. Liu, C.-X. Zhuo,
Z.-Q. Rong, K.-Y. Ye,
S.-L. You* _____ 4455–4458

Iridium-Catalyzed Intramolecular Asymmetric Allylic Dearomatization of Phenols

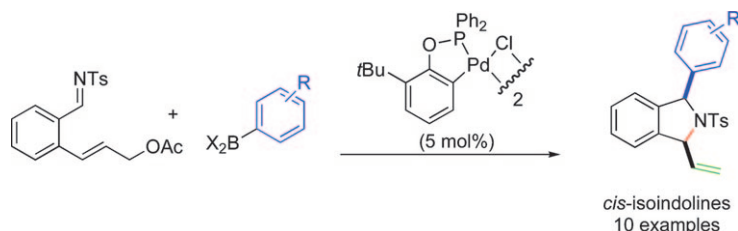


Cascade Reactions

F. J. Williams, E. R. Jarvo* — 4459–4462



Palladium-Catalyzed Cascade Reaction for the Synthesis of Substituted Isoindolines



Arylate then cyclize: A palladium(II)-catalyzed cascade sequence has been developed to provide highly diastereomerically enriched *cis*-1-aryl-3-vinyl isoidolines (see scheme). The method uses com-

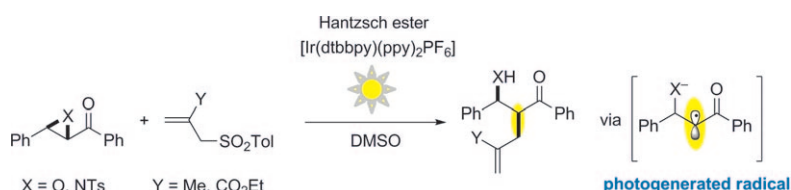
mercially available aryl boronic acids and boroxine compounds containing a variety of electron-rich, -neutral, or -poor aromatic groups. Ts = 4-toluenesulfonyl.

Photoredox Catalysis

M.-H. Larraufie, R. Pellet, L. Fensterbank,* J.-P. Goddard, E. Lacôte, M. Malacria, C. Ollivier* — 4463–4466



Visible-Light-Induced Photoreductive Generation of Radicals from Epoxides and Aziridines



It's a trap! Both epoxides and aziridines substituted by an aryl ketone can be reduced efficiently using visible-light photoredox catalysts. The radicals generated were trapped by allyl sulfones, and

formed α -branched β -hydroxy or amino derivatives with high diastereocontrol (see scheme; dtbbpy = 4,4'-di-*tert*-butyl-2,2'-bipyridine, ppy = 2-phenylpyridine).

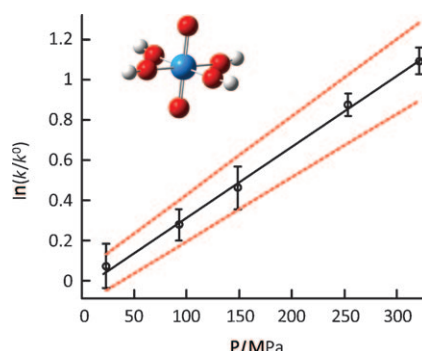
Reaction Kinetics

S. J. Harley, C. A. Ohlin, R. L. Johnson, A. F. Panasci, W. H. Casey* — 4467–4469



The Pressure Dependence of Oxygen Isotope Exchange Rates Between Solution and Apical Oxygen Atoms on the $[\text{UO}_2(\text{OH})_4]^{2-}$ Ion

Under pressure: The pressure dependence of isotope exchange rate was determined for apical oxygen atoms in the $[\text{UO}_2(\text{OH})_4]^{2-}(\text{aq})$ ion (see picture). The results can be interpreted to indicate an associative character of the reaction.

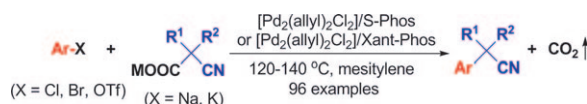


Cross-Coupling

R. Shang, D.-S. Ji, L. Chu, Y. Fu, L. Liu* — 4470–4474

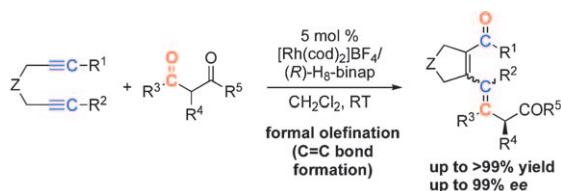


Synthesis of α -Aryl Nitriles through Palladium-Catalyzed Decarboxylative Coupling of Cyanoacetate Salts with Aryl Halides and Triflates



Worth its salt: The palladium-catalyzed decarboxylative coupling of the cyanoacetate salt as well as its mono- and disubstituted derivatives with aryl chlorides, bromides, and triflates is described (see scheme). This reaction is potentially

useful for the preparation of a diverse array of α -aryl nitriles and has good functional group tolerance. S-Phos = 2-(2,6-dimethoxybiphenyl)dicyclohexylphosphine, Xant-Phos = 4,5-bis(diphenylphosphino)-9,9-dimethylxanthene.



A cationic rhodium(I) complex catalyzes the title reaction of 1,6-diynes through a [2+2+2] cycloaddition and subsequent electrocyclic ring opening (see scheme; cod = 1,5-cyclooctadiene, H₈-binap = 2,2'-

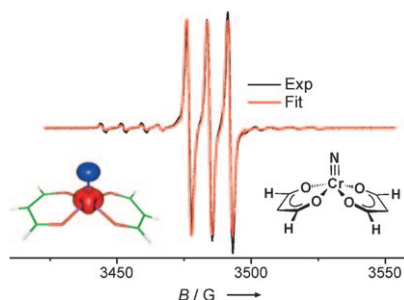
bis(diphenylphosphino)-5,5',6,6',7,7',8,8'-octahydro-1,1'-binaphthyl). The asymmetric intramolecular [2+2+2] cycloaddition of 1,3-dicarbonyl compounds with 1,6-enynes was also accomplished.

Asymmetric Catalysis

T. Suda, K. Noguchi,
K. Tanaka* 4475 – 4479

Rhodium-Catalyzed Asymmetric Formal Olefination or Cycloaddition: 1,3-Dicarbonyl Compounds Reacting with 1,6-Diynes or 1,6-Enynes

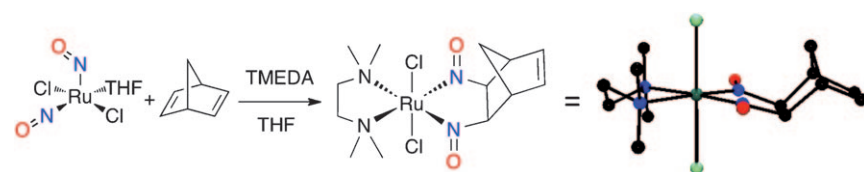
Longer, yet stronger: Terminal chromium(V) nitride complexes (see picture) react with low-valent platinum-metal complexes as well as with main-group Lewis acids to yield nitride-bridged systems. Rigorous fitting of the EPR data shows that the superhyperfine coupling of the chromium(V) center with the ¹⁴N nuclear spin approximately doubles in response to the formation of a Cr–N bridge. This effect also exists in computations for the hypothetical lengthening of the Cr–N bond.



EPR Spectroscopy

J. Bendix,* C. Anthon,
M. Schau-Magnussen,
T. Brock-Nannestad, J. Vibenholt,
M. Rehman, S. P. A. Sauer – 4480 – 4483

Heterobimetallic Nitride Complexes from Terminal Chromium(V) Nitride Complexes: Hyperfine Coupling Increases with Distance



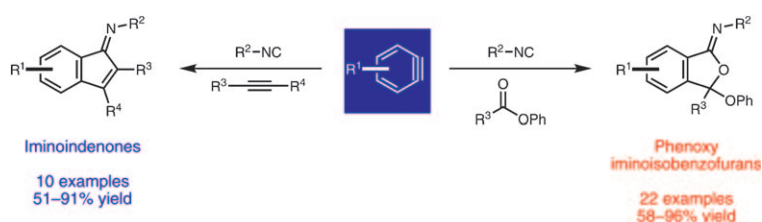
Unruly NO more: The synthesis of [RuCl₂(NO)₂(THF)] has been achieved by the reaction of [(cymene)RuCl₂]₂ with NO in THF. In the presence of a chelating

L₂-type ligand [RuCl₂(NO)₂(THF)] binds alkenes to its nitrosyl nitrogen atoms (see scheme).

Ligand-Based Reactivity

M. R. Crimmin, R. G. Bergman,*
F. D. Toste* 4484 – 4487

Synthesis of [RuCl₂(NO)₂(THF)] and its Double C–N Bond-Forming Reactions with Alkenes



Multicomponent Reactions

K. M. Allan, C. D. Gilmore,
B. M. Stoltz* 4488 – 4491

Benzannulated Bicycles by Three-Component Aryne Reactions

Triple crown: A pair of three-component coupling reactions between arynes, isocyanides, and either activated alkynes or phenyl esters generates unusual iminoindenes or phenoxy iminoisobenzofurans (see scheme), the latter of which may be

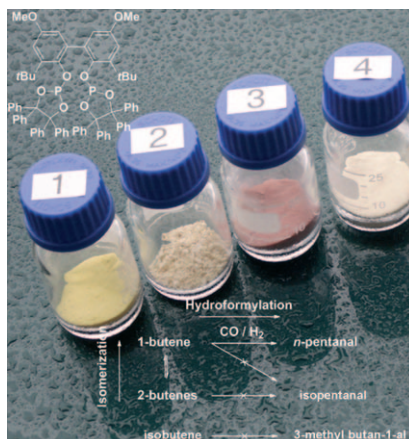
advanced to *o*-ketobenzamides by performing direct hydrolysis. The synthetic utility of these compounds is demonstrated in a rapid preparation of substituted dibenzoketocaprolactams.

Hydroformylation

M. Jakuttis, A. Schönweiz, S. Werner,
R. Franke, K.-D. Wiese, M. Haumann,*
P. Wasserscheid* — 4492 – 4495



Rhodium–Phosphite SILP Catalysis for the
Highly Selective Hydroformylation of
Mixed C₄ Feedstocks



The cat. that got the butene: Highly active and selective diphosphite ligands are applied for rhodium-catalyzed supported ionic liquid phase (SILP) hydroformylation and make it possible to form linear *n*-pentanal with exceptional selectivity from a mixed butene feedstock by combined isomerization and hydroformylation (see picture, vials 1–4 show typical SILP catalysts employed in this study.). The SILP catalyst is stable for more than 800 h on stream.

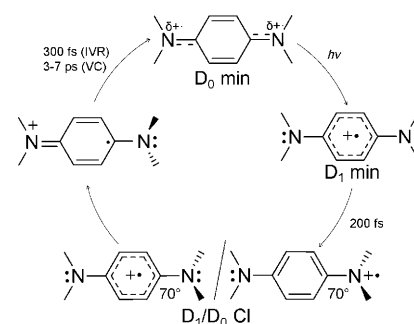
Ultrafast Processes

J. Grilj, E. N. Laricheva, M. Olivucci,*
E. Vauthey* — 4496 – 4498



Fluorescence of Radical Ions in Liquid
Solution: Wurster's Blue as a Case Study

The fluorescence lifetime of the radical cation of *N,N,N',N'*-tetramethyl-*p*-phenylenediamine (Wurster's blue) decreases from 260 ps at 82 K to 200 fs at room temperature. Calculations indicate a small barrier between the excited-state minimum (D₁ min) and a conical intersection (CI) of the excited and ground state potentials. The intersection is reached within 200 fs upon torsion of one of the C–N bonds.



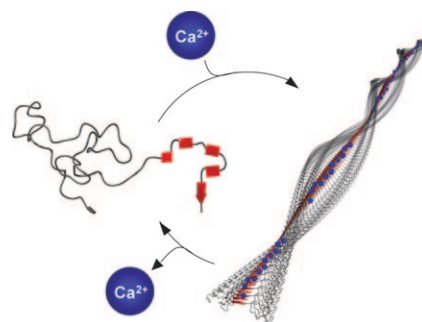
Bioconjugate Self-Assembly

R. I. Kühnle, H. G. Börner* — 4499 – 4502



Calcium Ions to Remotely Control the
Reversible Switching of Secondary and
Quaternary Structures in Bioconjugates

A biomimetic strategy to modulate inter- and intramolecular Coulomb interactions of peptides allows for the reversible regulation of functions of peptide–polymer conjugates. Calcium ions are exploited as triggers to screen peptide charges, thereby switching the peptide secondary structure. This approach results in a reversible control mechanism for bioconjugate self-assembly. Disassembly is feasible by regulating the Ca²⁺ levels using competitive Ca²⁺ binders.

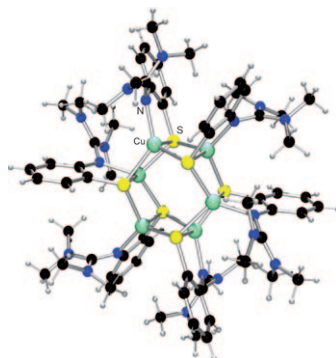


Copper Sulfur Clusters

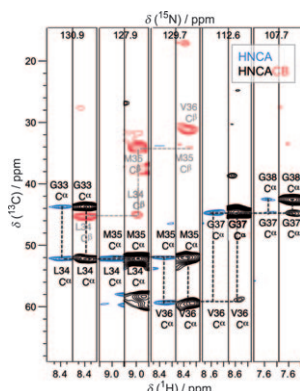
A. Neuba, U. Flörke, W. Meyer-Klaucke,
M. Salomone-Stagni, E. Bill, E. Bothe,
P. Höfer, G. Henkel* — 4503 – 4507



The Trinuclear Copper(I) Thiolate
Complexes [Cu₃(NGuaS)₃]^{0/1+} and their
Dimeric Variants [Cu₆(NGuaS)₆]^{1+/2+/3+}
with Biomimetic Redox Properties



A mixed-valent redox-active copper thiolate complex is formed in the reaction of [Cu(MeCN)₄]PF₆ with a CPh₃ thioether by a combination of homo- and heterolytic cleavage of the S–CPh₃ bond. In its oxidized state, the hexanuclear copper sulfur cluster (see picture) has the same average metal oxidation state as the dinuclear copper thiolate center of cytochrome c oxidase or N₂O reductase.



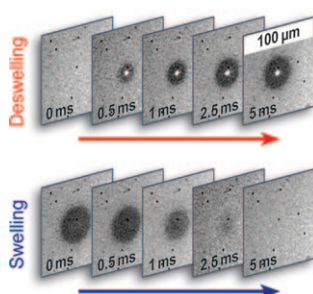
Structural characterization of insoluble proteins often relies on solid-state NMR spectroscopy. Perdeuteration and partial back-substitution of exchangeable protons, as proposed for crystalline model proteins, is now shown to lead to beneficial proton spectra for heterogeneous systems, such as fibrils formed by the Alzheimer's disease β -amyloid peptide A β 40, the lipid reconstituted β -barrel membrane protein OmpG, and the α -helical membrane protein bacteriorhodopsin.

Protein Analysis



R. Linser, M. Dasari, M. Hiller, V. Higman, U. Fink, J.-M. Lopez del Amo, S. Markovic, L. Handel, B. Kessler, P. Schmieder, D. Oesterhelt, H. Oschkinat,*
B. Reif* _____ **4508–4512**

Proton-Detected Solid-State NMR Spectroscopy of Fibrillar and Membrane Proteins



Laser-stimulated polymer brushes: The temperature-dependent switching kinetics of surface-grafted thermoresponsive polymer brushes were investigated by a stroboscopic micromanipulation/characterization technique for real-time parallel measurements (see picture). Intrinsic response times range from the microsecond to the millisecond time scale; these results could lead to fabrication of nanosized polymeric actuators and sensors with unprecedented responsivities.

Stroboscopic Laser Techniques



C. Amiri Naini, S. Franzka, S. Frost, M. Ulbricht, N. Hartmann* **4513–4516**

Probing the Intrinsic Switching Kinetics of Ultrathin Thermoresponsive Polymer Brushes



Supporting information is available on www.angewandte.org (see article for access details).



A video clip is available as Supporting Information on www.angewandte.org (see article for access details).



This article is available online free of charge (Open Access)

Sources

Product and Company Directory

You can start the entry for your company in "Sources" in any issue of *Angewandte Chemie*.

If you would like more information, please do not hesitate to contact us.

Wiley-VCH Verlag – Advertising Department

Tel.: 0 62 01 - 60 65 65

Fax: 0 62 01 - 60 65 50

E-Mail: MSchulz@wiley-vch.de

Service

Spotlight on Angewandte's
Sister Journals _____ **4256–4258**

Preview _____ **4517**